BABEŞ–BOLYAI UNIVERSITY
Faculty of Chemistry and Chemical Engineering

UNIVERSITÄT LEIPZIG
Department of Chemistry and Mineralogy

THEORETICAL STUDY OF MAIN GROUP ELEMENTS AND THEIR COMPLEXES WITH TRANSITION METALS

Ph.D. Thesis Abstract

Scientific advisors

Prof. Dr. Ioan Silaghi-Dumitrescu

Prof. Dr. Luminiţa Silaghi-Dumitrescu

Prof. Dr. Evamarie Hey-Hawkins

Ph.D. student

Menyhárt-Botond Sárosi

Cluj-Napoca
–2011–

BABEŞ–BOLYAI UNIVERSITY
Faculty of Chemistry and Chemical Engineering

Menyhárt-Botond SÁROSI

THEORETICAL STUDY OF MAIN GROUP ELEMENTS AND THEIR COMPLEXES WITH TRANSITION METALS

Ph.D. Thesis Abstract

Jury

President:

Conf. Dr. Castelia CRISTEA	Babeş-Bolyai University

Reviewers:

Prof. Dr. Ion GROSU	Babeş-Bolyai University
Prof. Dr. R. Bruce KING	The University of Georgia
CŞI Dr. Ioan TURCU	I.N.C.D.T.I.M. Cluj-Napoca

Public defense: 30. September 2011.

Contents

Graphical abstract

1. Carbaborane-Substituted 1,2-Diphosphetanes

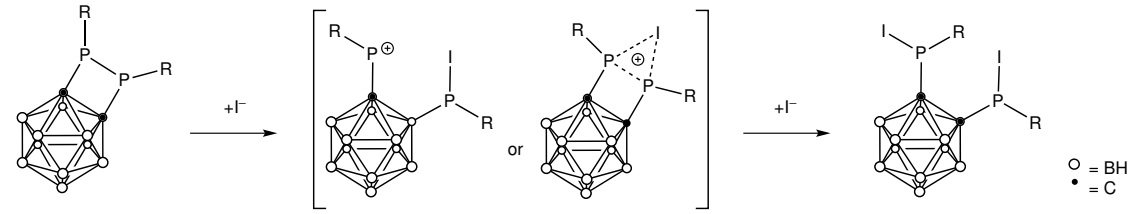

rac-**3**: R = $C(CH_3)_3$
rac-**4**: R = $N\{CH(CH_3)_2\}_2$

a/**b**-P^+ **a**/**b**-I^+
theoretical ionic reaction intermediates

rac-**5**: R = $C(CH_3)_3$
rac-, *meso*-**6**: R = $N\{CH(CH_3)_2\}_2$

2. Transition metal carbonyl sulfides

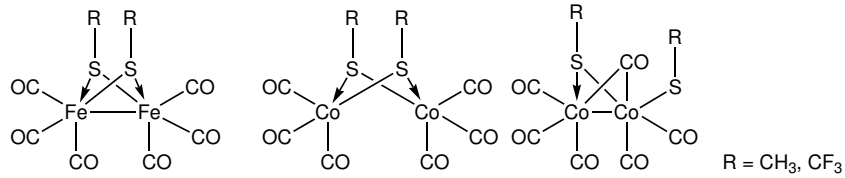

alkylthio iron carbonyls **alkylthio cobalt carbonyls**

R = CH_3, CF_3

3. Transition metal nitrosyl sulfides

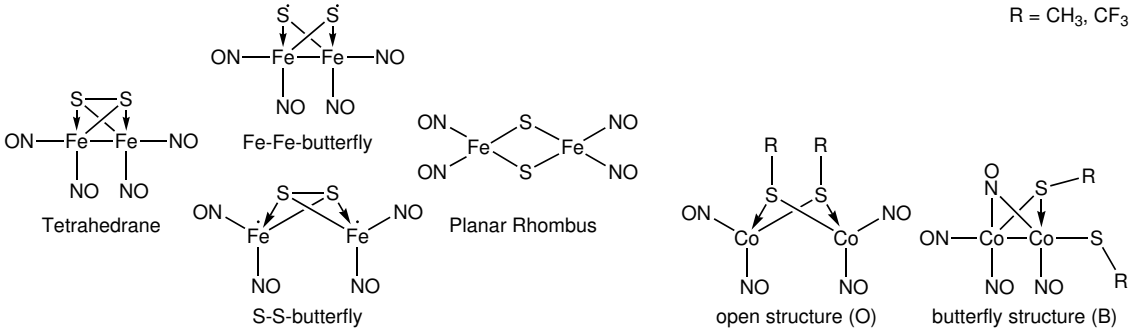

alkylthio iron nitrosyls **alkylthio cobalt nitrosyls**

4. Unsymmetrical dinuclear rhodium complexes

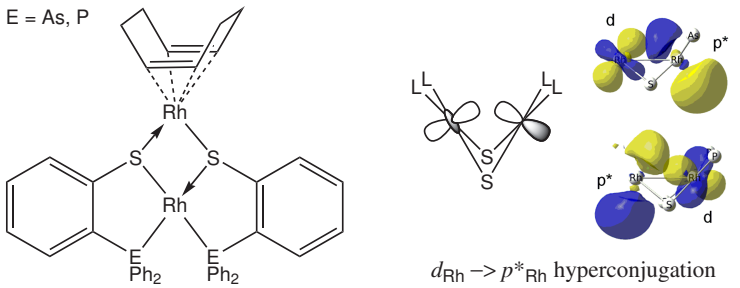

$d_{Rh} \rightarrow p^*_{Rh}$ hyperconjugation

Abstract

This Ph.D. thesis presents results in selected areas of main group element and transition metal chemistry, where theoretical investigations lead to a deeper understanding of the proposed problems. In the first chapter, the substituent dependent diastereoselective behavior of carbaborane-substituted 1,2-diphosphetanes is addressed. The second and third chapters present results and highlight unsolved topics in the long known field of organosulfur transition metal carbonyl derivatives and transition metal nitrosyl sulfides. And last, but not least, the electronic structure and intramolecular interactions of arsanylaryl- and phosphanylarylthiol ligated transition metal complexes are discussed in the fourth chapter.

Keywords: 1,2-diphosphetanes, carbaboranes, iron, cobalt, alkylthio metal carbonyls, alkylthio metal nitrosyls, dinuclear rhodium complexes, density functional theory

1. Carbaborane-Substituted 1,2-Diphosphetanes

1.1. Introduction

Compounds **3** and **4** react with elemental iodine to give the first 1,2-bis(iodophosphanyl)-1,2-dicarba-closo-dodecaborane(12) compounds **5** and **6** (Figure 1). In the case of **3**, the ring-opening reaction is diastereoselective to give the *rac* diastereomer **5** exclusively while the reaction of 4 with iodine results in formation of both diastereomers. This different diastereoselective behavior has been investigated with density functional theory (DFT) methods.

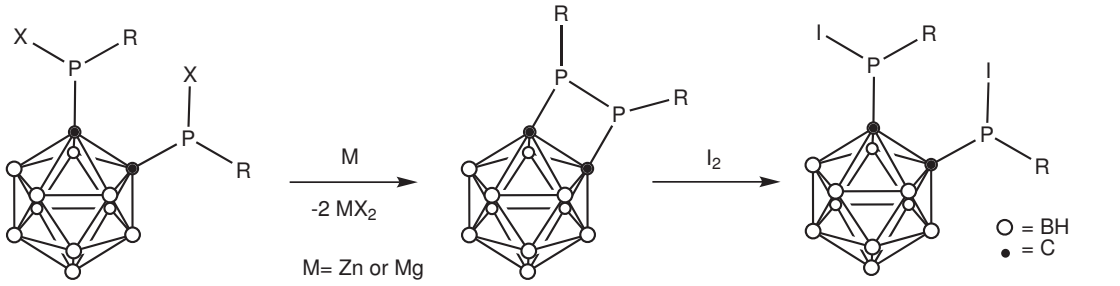

rac-, *meso*-**1**: X = Cl; R = $C(CH_3)_3$
rac-, *meso*-**2**: X = Br; R = $N\{CH(CH_3)_2\}_2$

rac-**3**: R = $C(CH_3)_3$
rac-**4**: R = $N\{CH(CH_3)_2\}_2$

rac-**5**: R = $C(CH_3)_3$
rac-, *meso*-**6**: R = $N\{CH(CH_3)_2\}_2$

Figure 1 – Synthesis of 1,2-diphosphetanes rac-**3** and rac-**4** and their subsequent ring-opening reactions.

1.3. Original contributions

Table 3 summarizes the B3LYP/6-311G** relative energies for all of the optimized structures. The *rac* forms of **3** and **4** are clearly energetically favored by approximately 10 kcal mol^{-1}, which is in agreement with the experiments. However, the energy difference between the *rac*/*meso* forms of **5** and **6** is too insignificant (around 1 kcal mol^{-1}) to suggest an energetic preference for one of the isomers.

The transition states (TSs) corresponding to the pyramidal inversion of one of the P atoms for both reagents (**TS3**, **TS4**) and products (**TS5**, **TS6**) lie at significantly

higher relative energy values, suggesting a considerable energy barrier (Table 3). Thus, the conformational rearrangement must occur at the reaction intermediates, which can reasonably be considered as one of the ionic compounds depicted in Figure 5. The energy difference between the *trans*/*cis* forms of both alkyl- and amido-substituted intermediates is again insignificant (Table 3).

Table 3 − B3LYP/6-311G** relative energies (with zero-point energy corrections, kcal mol^{-1}) and imaginary frequencies (cm^{-1}) of the studied carbaborane-substituted 1,2-diphosphetanes.

Reactants		**Products**		**Theoretical intermediates** R = $C(CH_3)_3$		R = $N\{CH(CH_3)_2\}_2$	
***rac*-3**	0.0	***rac*-5**	0.0	***trans*-a P^+**	0.0	***trans*-b I^+**	0.0
***meso*-3**	10.0	***meso*-5**	1.5	***cis*-a P^+**	3.1	***cis*-b I^+**	0.5
TS3	35.5 [299*i*]	**TS5**	51.3 [198*i*]	***cis*-a I^+**	9.7	***trans*-b P^+**	2.8
***rac*-4**	0.0	***rac*-6**	0.0	***trans*-a I^+**	10.6	***cis*-b P^+**	5.3
***meso*-4**	11.9	***meso*-6**	1.1	**TSa P^+**	27.9 [240*i*]	**TSb P^+**	12.9 [16*i*]
TS4	35.9 [294*i*]	**TS6**	34.0 [311*i*]	**TSa I^+**	50.2 [353*i*]	**TSb I^+**	18.1 [29*i*]

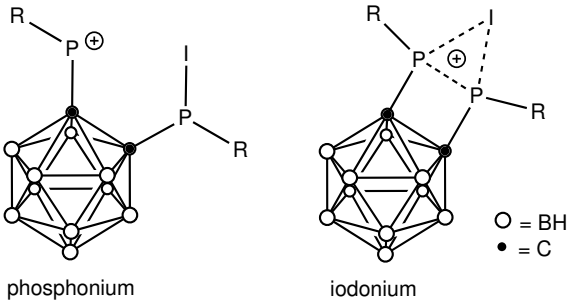

Figure 5 – The theoretically considered ionic intermediates.

The energy barriers to inversion obtained for the amido-substituted intermediates **TSb P^+** and **TSb I^+** are almost three times lower than the barriers predicted for the alkyl-substituted intermediates (**TSa P^+** and **TSa I^+**). It seems that the conformational rearrangement can take place at the amido-substituted intermediates, resulting in the experimentally observed *rac*/*meso* mixture of **6**, while the alkyl-substituted intermediates possess higher energy barriers to such conformational changes. It cannot be excluded that the present $n_N \rightarrow \sigma^*_{(P–A)}$ hyperconjugations (Figure 9) are responsible for the observed lowering of the inversion barrier.

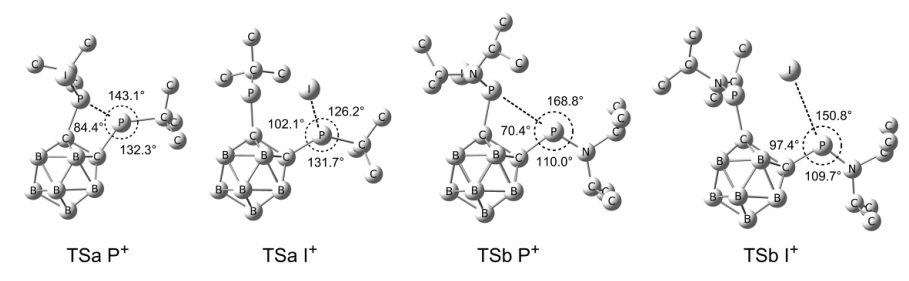

Figure 7 – Transition state geometries for the inversion at one of the P atoms of the ionic intermediates. (H atoms are not shown).

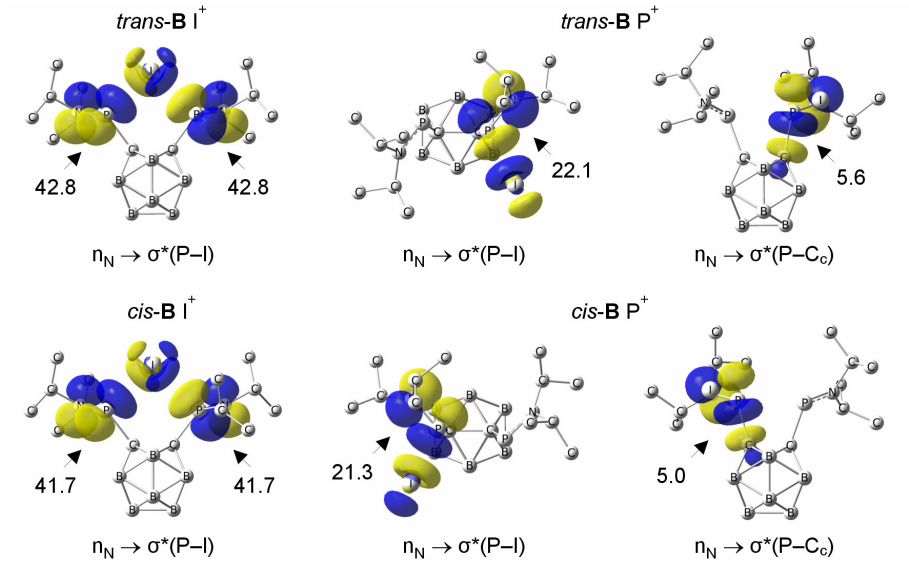

Figure 9 – Hyperconjugation of the occupied lone pair at nitrogen (n_N) with the unoccupied anti-bonding orbital between the adjacent phosphorus and its substituent (σ*(P–A)) for the amido-substituted intermediates. Numbers represent the second-order energy-lowering values in kcal mol^{-1} (contours at isovalue 0.07; hydrogen atoms are not shown).

1.4. Conclusions

Theoretical calculations indicate that the *rac* to *meso* conformational rearrangement can take place at the amido-substituted intermediates, resulting in the experimentally observed *rac*/*meso* mixture, while the alkyl-substituted intermediates possess higher energy barriers to such rearrangement.

2. Transition metal carbonyl sulfides

2.2.1. Experimental and theoretical data on iron carbonyl sulfides *(literature data)*

2.2.2. Original contributions

The six initial singlet geometries for $Fe_2(CO)_6(\mu\text{-}SCH_3)_2$ were optimized (Figure 15) and their vibrational frequencies were calculated according to the methodology described in chapter 2.4. The predicted energy differences between the corresponding non-planar structures with eclipsed and staggered $Fe(CO)_3$ units are 6.5 ± 1 kcal mol^{-1}, which is much lower than the 13.0 kcal mol^{-1} determined by Tye *et al*.[42] Both basis sets predict very similar trends for the relative energies of the six $Fe_2(CO)_6(\mu\text{-}SCH_3)_2$ isomers (Figure 18).

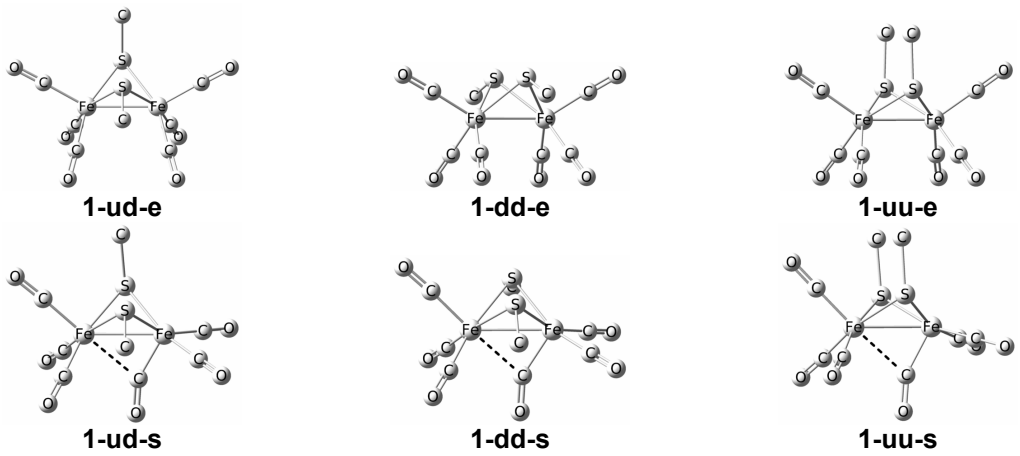

Figure 15 – BP86/6-31G(d) optimized $Fe_2(CO)_6(\mu\text{-}SR)_2$ geometries with out-of-plane carbonyl moieties. The hydrogen and fluorine atoms have been omitted for the sake of clarity.

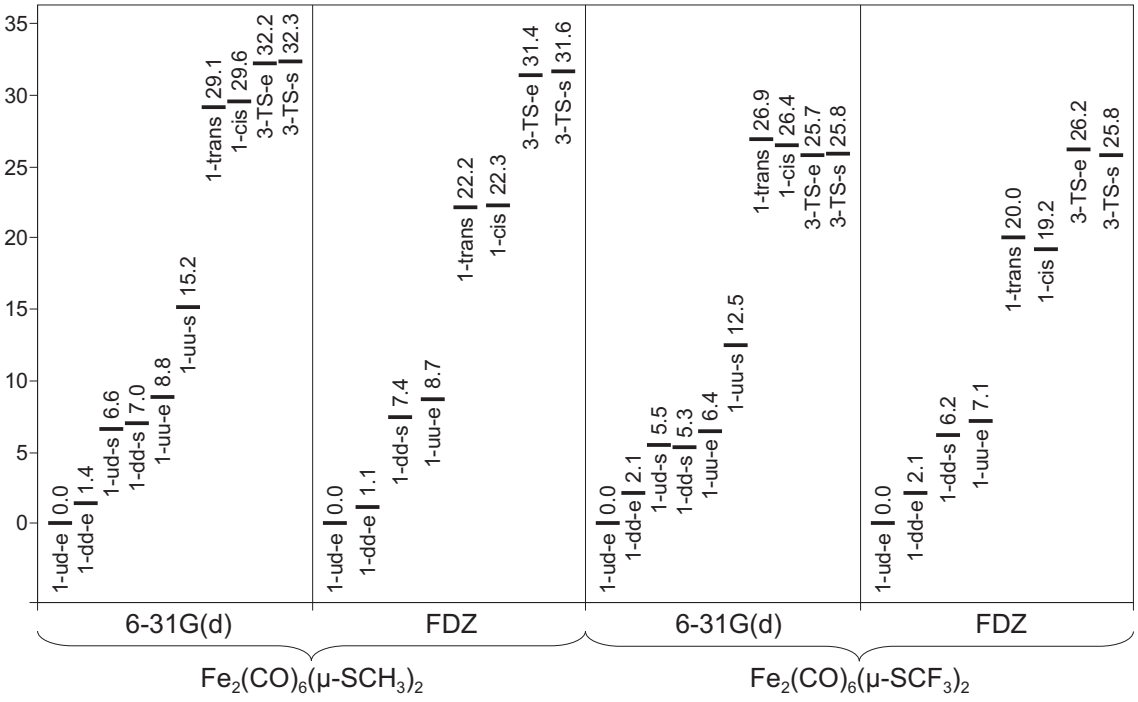

Figure 18 – Relative energies in kcal mol^{-1} of the optimized $Fe_2(CO)_6(\mu\text{-}SR)_2$ singlet geometries.

Additionally, two high energy singlet $Fe_2(CO)_6(\mu\text{-}SCH_3)_2$ structures were also located by both methods (Figure 16). The relative energies of the **1-trans** and **1-cis** structures are significantly higher, than the relative energies of the corresponding **1-ud-e** global minima.

Figure 16 – BP86/6-31G(d) optimized $Fe_2(CO)_6(\mu\text{-}SR)_2$ geometries with in-plane carbonyl moieties. The hydrogen and fluorine atoms have been omitted for the sake of clarity.

The transition states for the inversion of the non-planar Fe_2S_2 butterfly structures with both eclipsed and staggered carbonyl groups were identified as the triplet **3-TS-e** and **3-TS-s** structures (Figure 17). Both transitions states are predicted as the highest relative energy isomer.

Figure 17 – BP86/6-31G(d) transition state geometries for the inversion of non-planar Fe_2S_2 structures. The hydrogen and fluorine atoms have been omitted for the sake of clarity.

Geometry optimization of $Fe_2(CO)_6(\mu\text{-}SCF_3)_2$ structures yielded the same relative energy ordering of the isomers (Figure 18) and very similar structural parameters as the methyl-substituted compounds (Table 10). This indicates that the electronegativity of the RS group has little effect on the relative energies of the stereoisomers. However, in contrast to its methyl-substituted pair, the **1-dd-s** $Fe_2(CO)_6(\mu\text{-}SCF_3)_2$ structure with staggered $Fe(CO)_3$ moieties is now predicted by BP86/FDZ as a local minimum. This might indicate that, the more electronegative SR group provides additional stability for the $Fe_2(CO)_6(\mu\text{-}SR)_2$ structures with staggered $Fe(CO)_3$ moieties.

Using the global minima for both methyl- and trifluoromethyl-substituted $Fe_2(CO)_6(\mu\text{-}SR)_2$ structures (**1-ud-e**), bond dissociation energies for the loss of one carbonyl group have been calculated (Figure 19).

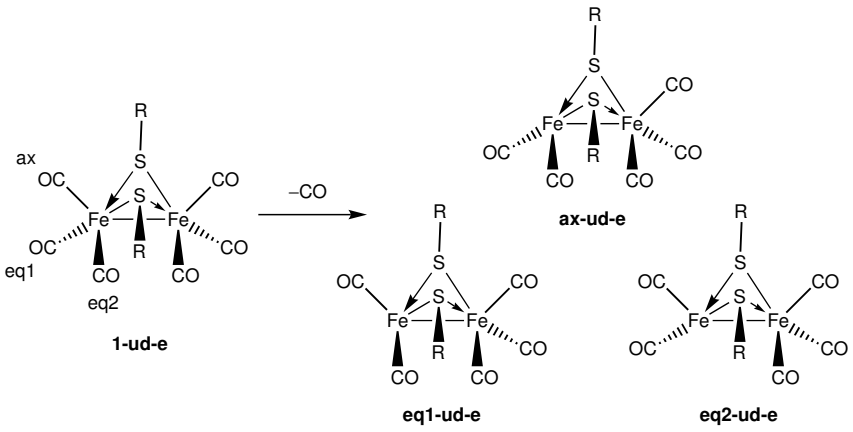

Figure 19 – Decarbonylation of **1-ud-e** $Fe_2(CO)_6(\mu\text{-}SR)_2$.

The predicted single carbonyl dissociation energy for the $Fe_2(CO)_6(\mu\text{-}SCH_3)_2$ **1-ud-e** structure is around 55 kcal mol^{-1} by BP86/6-31G(d) and around 50 kcal mol^{-1} by BP86/FDZ. The dissociation energy for the corresponding $Fe_2(CO)_6(\mu\text{-}SCF_3)_2$ **1-ud-e** structure is predicted to be very similar: around 52 kcal mol^{-1} by BP86/6-31G(d) and around ~48 kcal mol^{-1} by BP86/FDZ. The energy required for further carbonyl dissociation from $(SR)_2Fe_2(CO)_5$ to give $(SR)_2Fe_2(CO)_4$ + CO is considerably lower for both methyl- and trifluoromethyl-substituted species. It is predicted to be roughly 38 kcal mol^{-1} by BP86/6-31G(d) and around 34 kcal mol^{-1} by BP86/FDZ (Table 12). Thus, $(SR)_2Fe_2(CO)_6$ appears to be more stable with respect to extrusion of a carbonyl ligand, than the pentacarbonyl derivatives are.

Table 12 –Dissociation energies (kcal mol^{-1}) for the successive removal of carbonyl groups from the $(SR)_2Fe_2(CO)_n$ (n = 4, 5, 6) derivatives based on the lowest energy structures (BP86/6-31G(d) values in normal font; BP86/FDZ values in *italics*).

	Me		**CF_3**	
$(SR)_2Fe_2(CO)_6 \rightarrow (SR)_2Fe_2(CO)_5$ + CO				
1-ud-e → **ax-ud-e** + CO	54.3	*50.1*	52.9	*48.4*
1-ud-e → **eq1-ud-e** + CO	53.9	*47.9*	53.8	*48.6*
1-ud-e → **eq2-ud-e** + CO	56.6	*50.7*	47.8	*45.7*
$(SR)_2Fe_2(CO)_5 \rightarrow (SR)_2Fe_2(CO)_4$ + CO				
ax-ud-e → **4CO-trans** + CO	38.5	*33.9*	36.9	*33.4*
eq1-ud-e → **4CO-trans** + CO	38.9	*36.1*	35.9	*33.2*
eq2-ud-e → **4CO-trans** + CO	36.1	*33.3*	42.0	*36.1*

2.2.3. Conclusions

Structures with central planar Fe_2S_2 units and 180° S–Fe–Fe–S dihedral angles were also found for $Fe_2(CO)_6(\mu\text{-}SR)_2$ derivatives, but always at significantly higher energies than the butterfly structures. Additionally, the transition states for the inversion of the non-planar $Fe_2(CO)_6(\mu\text{-}SR)_2$ structures through planar geometries were also located. Their relative energy range of 26 to 32 kcal mol^{-1} suggests a considerably inversion barrier.

The FDZ basis set was able to identify subtle differences between methyl- and trifluoromethyl-substituted $Fe_2(CO)_6(\mu\text{-}SR)_2$ systems.

The bond dissociation energies for the successive loss of one carbonyl group from the $Fe_2(CO)_n(\mu\text{-}SR)_2$ structures, suggest that the hexacarbonyl derivatives are more stable with respect to extrusion of a carbonyl ligand, than the pentacarbonyl derivatives.

2.3.1. Experimental and theoretical data on cobalt carbonyl sulfides *(literature data)*

2.3.2. Original contributions

The optimized $Co_2(CO)_6(SR)_2$ (R = CH_3, CF_3) geometries are shown on Figure 25. All of these structures have very similar energies, lying within 8 kcal mol^{-1} of each other (Figure 26). All calculations were carried out as described in chapter 2.4. However, only the results obtained with the BP86/FDZ method will be presented.

The $Co_2(CO)_6(SCF_3)_2$ system is rather different from the $Co_2(CO)_6(SCH_3)_2$ system since the lowest lying structure is not one of the open geometries but instead the **B-ud** butterfly isomer. There thus appears to be a greater preference for metal–metal bonding in the $Co_2(CO)_6(SCF_3)_2$ structures than in the $Co_2(CO)_6(SCH_3)_2$ structures. However, the electronegativity of the SR group does not seem to have a high impact on the geometrical parameters of both the butterfly and open $Co_2(CO)_6(SR)_2$ stereoisomers, as indicated by the very similar Co···Co and Co–S distances in both $Co_2(CO)_6(SCF_3)_2$ and $Co_2(CO)_6(SCH_3)_2$ structures (Table 14). However, the effect of the SR groups nature is felt in the atomic charge distributions.

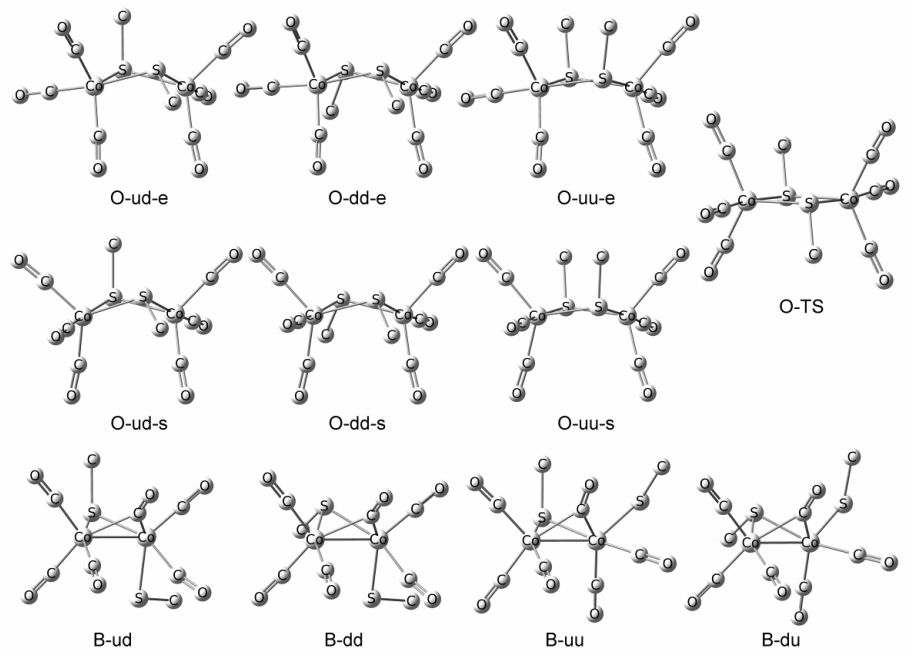

Figure 25 – The 11 optimized $Co_2(CO)_6(SR)_2$ structures (R = CH_3 or CF_3). The hydrogen and fluorine atoms have been omitted for the sake of clarity.

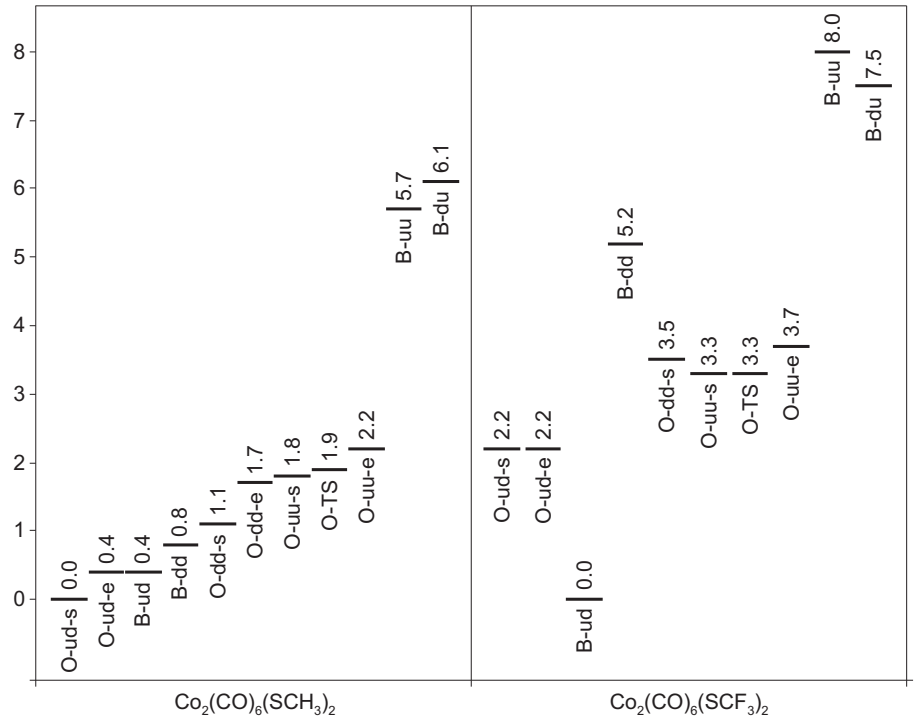

Figure 26 – Relative energies in kcal mol^{-1} for the investigated $Co_2(CO)_6(SR)_2$ structures.

Table 14 – Calculated Co–Co and Co–S distances (Å), imaginary frequencies (cm^{-1}) and HOMO-LUMO gaps (eV) for the $Co_2(CO)_6(SR)_2$ structures.

	Co–Co		Co–S		imag. freq.		HOMO-LUMO	
	R=CH_3	**R=CF_3**	**R=CH_3**	**R=CF_3**	**R=CH_3**	**R=CF_3**	**R=CH_3**	**R=CF_3**
O-ud-s	3.359	3.387	2.314, 2.323, 2.342, 2.362	2.313, 2.315, 2.357, 2.360	none		1.6	1.6
O-ud-e	3.402	3.417	2.292, 2.369	2.292, 2,364	none		1.7	1.7
B-ud	2.523	2.523	2.242, 2.289, *2.363*	2.222, 2.278, *2.361*	none		1.8	1.5
B-dd	2.514	2.514	2.272, 2.288, *2.356*	2.262, 2.277, *2.350*	none		1.8	1.4
O-dd-s	3.402	3.457	2.326, 2.351	2.320, 2.358	none	8*i*	1.6	1.6
O-dd-e	3.419	–	2.299, 2.373	–	none	–	1.5	–
O-uu-s	3.393	3.433	2.320, 2.354	2.314, 2.360	none		1.5	1.6
O-TS	3.472	3.469	2.325, 2.347	2.320, 2.358	31*i*	16*i*	1.5	1.5
O-uu-e	3.396	3.436	2.305, 2.362	2.301, 2.363	none		1.7	1.8
B-uu	2.518	2.510	2.271, 2.296, *2.303*	2.269, 2.278, *2.296*	none		0.9	1.1
B-du	2.522	2.515	2.240, 2.311, *2.309*	2.257, 2.282, *2.303*	none		1.0	1.2

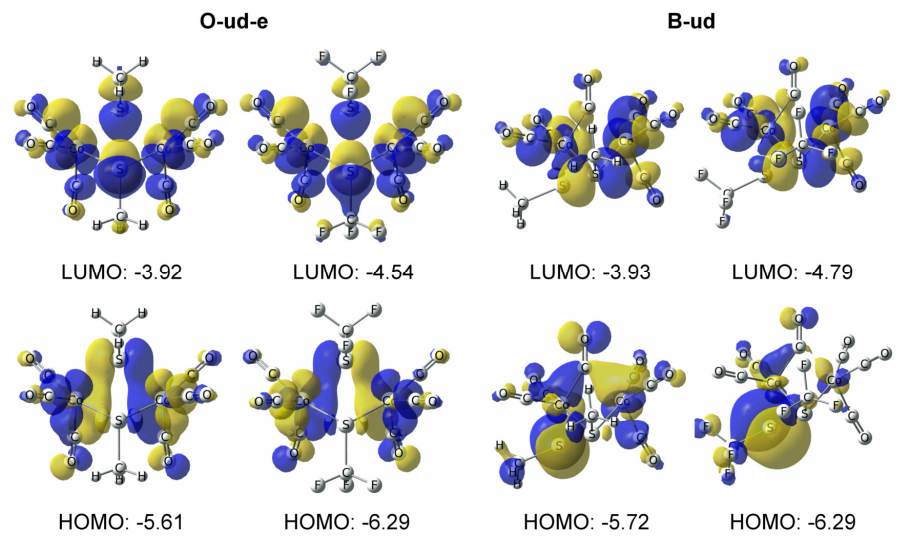

Figure 27 – Energies (eV) and contours at the 0.03 isovalue of the HOMO and LUMO of some relevant $Co_2(CO)_6(SR)_2$ structures (R = CH_3 or CF_3). + values: yellow; – values: blue.

Not only the geometries are not affected significantly by the nature of the SR group, but also the electronic structure of the corresponding conformers is influenced only weakly by it. Both the highest occupied (HOMO) and the lowest unoccupied molecular orbitals (LUMO) of the corresponding methyl or trifluoromethyl substituted **O-ud-e** and **B-ud** structures have very similar shapes and compositions (Figure 27).

Using the **O-ud-e** and **B-ud** structures, bond dissociation energies for the loss of one carbonyl group have been calculated for both methyl- and trifluoromethyl-substituted $Co_2(CO)_6(SR)_2$ species (Figure 28).

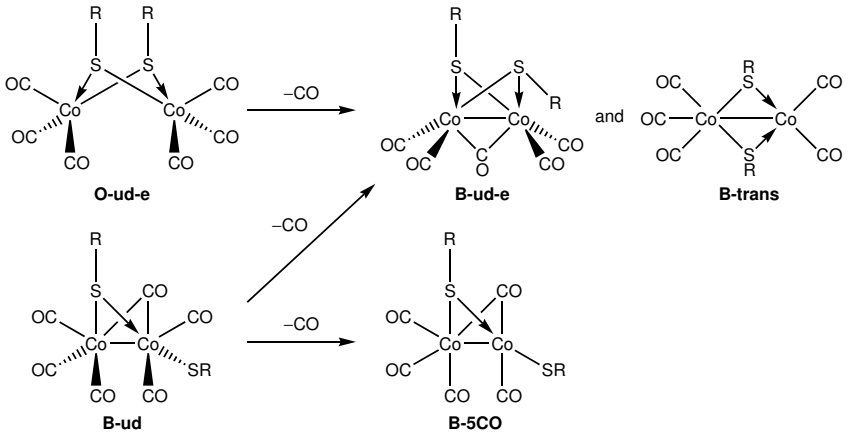

Figure 28 – Decarbonylation of the **O-ud-e** and **B-ud** $Co_2(CO)_6(SR)_2$ derivatives.

The predicted bond dissociation energy for the loss of one carbonyl group from the $Co_2(CO)_6(SR)_2$ **O-ud-e** structure is 14 kcal mol^{-1} for the methyl-substituted species and 17 kcal mol^{-1} for R = CF_3. The energy required for further carbonyl dissociation from $(SR)_2Co_2(CO)_5$ **B-ud-e** to give $(SR)_2Co_2(CO)_4$ + CO is considerably higher for both methyl- and trifluoromethyl-substituted species (Table 16).

Table 16 – Dissociation energies (kcal mol^{-1}) for the successive removal of carbonyl groups from the $(SR)_2Co_2(CO)_n$ (n = 4, 5, 6) derivatives based on the lowest energy structures.

Process	**Me**	**CF_3**
$(SR)_2Co_2(CO)_6$ [**O-ud-e**] → $(SR)_2Co_2(CO)_5$ [**B-ud-e**] + CO	14.0	*17.0*
$(SR)_2Co_2(CO)_6$ [**B-ud**] → $(SR)_2Co_2(CO)_5$ [**B-ud-e**] + CO	14.0	*19.2*
$(SR)_2Co_2(CO)_5$ [**B-ud-e**] → $(SR)_2Co_2(CO)_4$ [**O-4CO**] + CO	27.7	*29.0*

2.3.3. Conclusions

Density functional calculations on the $Co_2(CO)_6(SR)_2$ compounds (R= CH_3, CF_3) predict two different competing structure types. The lowest energy $Co_2(CO)_6(SCH_3)_2$ structure is an open isomer. However, this open isomer lies only 0.4 kcal mol^{-1} below the corresponding butterfly isomer. For the corresponding fluorinated derivative $Co_2(CO)_6(SCF_3)_2$ a greater preference towards direct metal–metal bonding exists.

The electronegativity of the RS group in the $Co_2(CO)_6(SR)_2$ structures has little effect on the main geometric parameters and the electronic structure of the corresponding conformers. However, it exerts a higher influence on the atomic charge distribution.

The bond dissociation energies for the successive loss of one carbonyl group from the $(SR)_2Co_2(CO)_6$ structures suggest that the hexacarbonyl derivatives are unstable with respect to extrusion of a carbonyl ligand, but most importantly, the resulting pentacarbonyl $(SR)_2Co_2(CO)_5$ derivatives are exclusively butterfly type structures with a direct Co–Co bond.

2.4. Theoretical methods

All of the optimizations were carried out in the gas phase using the BP86 density functional [77,78] of the Gaussian 03[86] and Gaussian 09[26] program packages. The first type of calculations were carried out using the standard 6-31G(d) basis set[82] for all atoms, while the second type of calculations used a custom basis set obtained by combining the Wachters primitive set[83] for Fe and Co, with the Dunning-Huzinaga basis set[85] augmented with a *d* polarization function for all other atoms. This combination of basis sets will be referred to as FDZ.

3. Transition metal nitrosyl sulfides

3.2. Theoretical methods

The general recommendation for conducting a DFT study of transition metal spin state energetics, is to compare at least a couple of different functionals including one of the nonhybrid type, which generally favor more covalent, spin-coupled descriptions, plus another from among the hybrid functionals, which typically favor more spin-polarized descriptions. [102] A functional giving intermediate results should also be considered. Thus, the following three functionals are used: (1) the pure BP86 functional,[77,78] (2) the hybrid B3LYP method,[24,25] and (3) the meta-GGA M06-L functional.[108,109] The 6-311G(d) basis set was used for all calculations.

3.3.1. Experimental and theoretical data on iron nitrosyl sulfides *(literature data)*

3.3.2. Original contributions

The nitrosyl analogue of the neutral $Fe_2(CO)_6S_2$, namely $Fe_2(NO)_4S_2$, has not yet been synthesized although it might be expected to be an oxidation product of Roussin's red dianion $Fe_2(NO)_4S_2^{2-}$.

The optimized geometries are shown on Figure 37, while their relative energies are summarized in Figure 38. As expected, BP86 and B3LYP give very different relative energy ordering for the structural isomers. The most obvious contradiction between the two methods is the predicted singlet–triplet splitting of the Fe- and S-butterfly structures. Not surprisingly, BP86 prefers the singlet state over the triplet one, while B3LYP predicts quite the opposite.

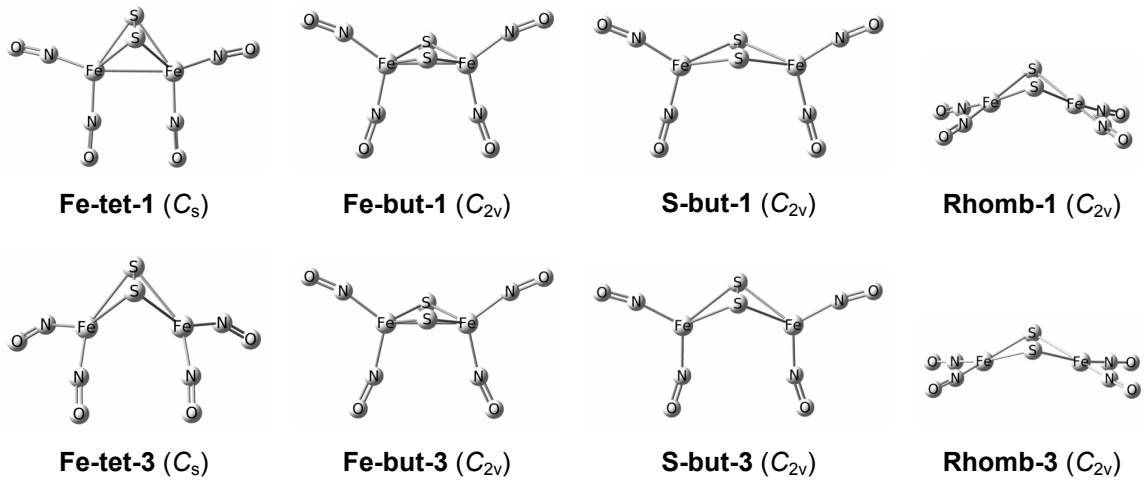

Figure 37 – B3LYP optimized singlet and triplet geometries of $Fe_2(NO)_4S_2$.

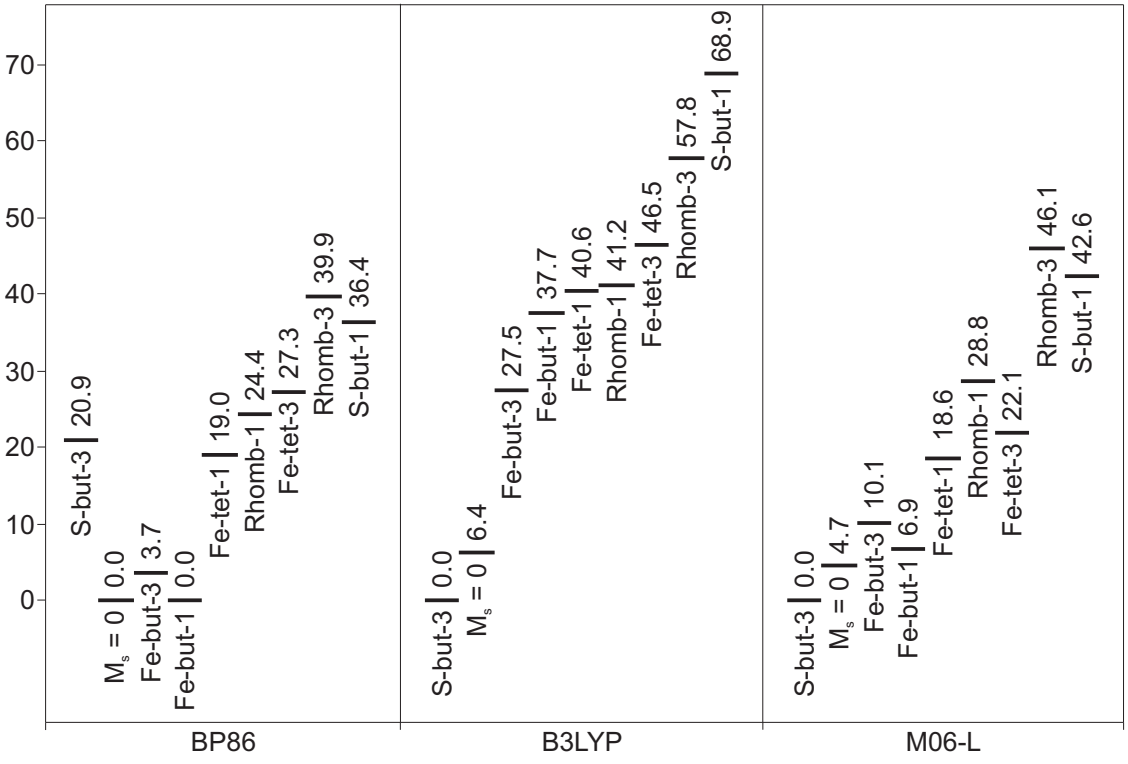

Figure 38 – Relative energies in kcal mol^{-1} of the optimized $Fe_2(NO)_4S_2$ geometries.

The M06-L results agree with the B3LYP ones. The M06-L functional also predicts the triplet diradical **S-but-3** isomer as the $Fe_2(NO)_4S_2$ ground state (Figure 38) and was able to predict the same antiferromagnitcally coupled broken symmetry solution as B3LYP (Figure 41).

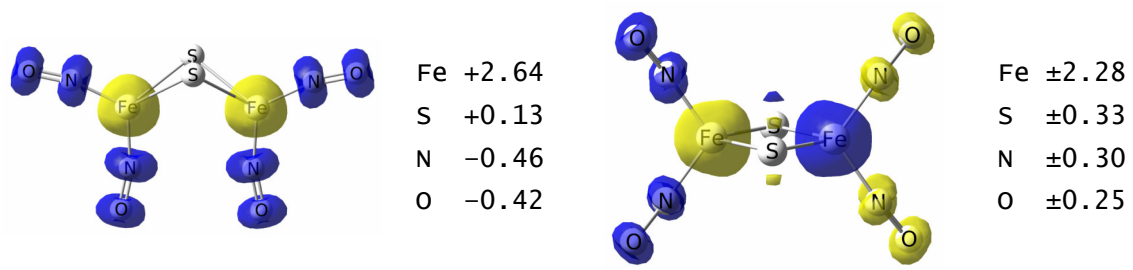

S-but-3 $\mathbf{M_s = 0}$

Figure 41 – M06-L geometries, spin density plots and values of $Fe_2(NO)_4S_2$ **S-but-3** and $\mathbf{M_s = 0}$. (isodensity value: 0.02; spin-up (+) regions are in yellow, spin-down (–) regions are in blue).

Since the M06-L functional confirms the B3LYP results, it is more probable that the correct theoretical ground state of the neutral species is the triplet diradical **S-but-3** and not the singlet diradical **Fe-but-1**. The presence of a triplet diradical ground state for the neutral $Fe_2(NO)_4S_2$ system could explain why it has not yet been synthesized.

3.3.3. Conclusions

Density functional calculations on the experimentally unknown $Fe_2(NO)_4(\mu\text{-}S)_2$ systems were carried out in an attempt to provide a clue to the chemical properties of this compound and why it has not yet been synthesized.

The results obtained using the B3LYP and M06-L functionals predicted a triplet S-butterfly structure as the $Fe_2(NO)_4(\mu\text{-}S)_2$ ground state. The presence of a triplet diradical ground state could play an important role in the extensively studied aggregation chemistry of the $[Fe_2(NO)_4S_2]^{2-}$ dianion, which leads to $Fe_4(NO)_7S_3^-$ and even higher Fe/NO/S clusters.[125,131,132]

3.4.1. Experimental and theoretical data on cobalt nitrosyl sulfides *(literature data)*

3.4.2. Original contributions

The chemistry of the cobalt analogs of Roussin's red salt esters, namely $Co_2(NO)_4(\mu\text{-}SR)_2$, has received much less attention than the chemistry of the related $[Fe_2(NO)_4S_2]^{2-}$ and $Fe_2(NO)_4(SR)_2$ derivatives.

The BP86 optimized geometries of the most relevant isomers are shown on Figure 46, while their relative energies predicted by all three functionals are summarized on Figure 48 in order to compare the performance of the three different methods.

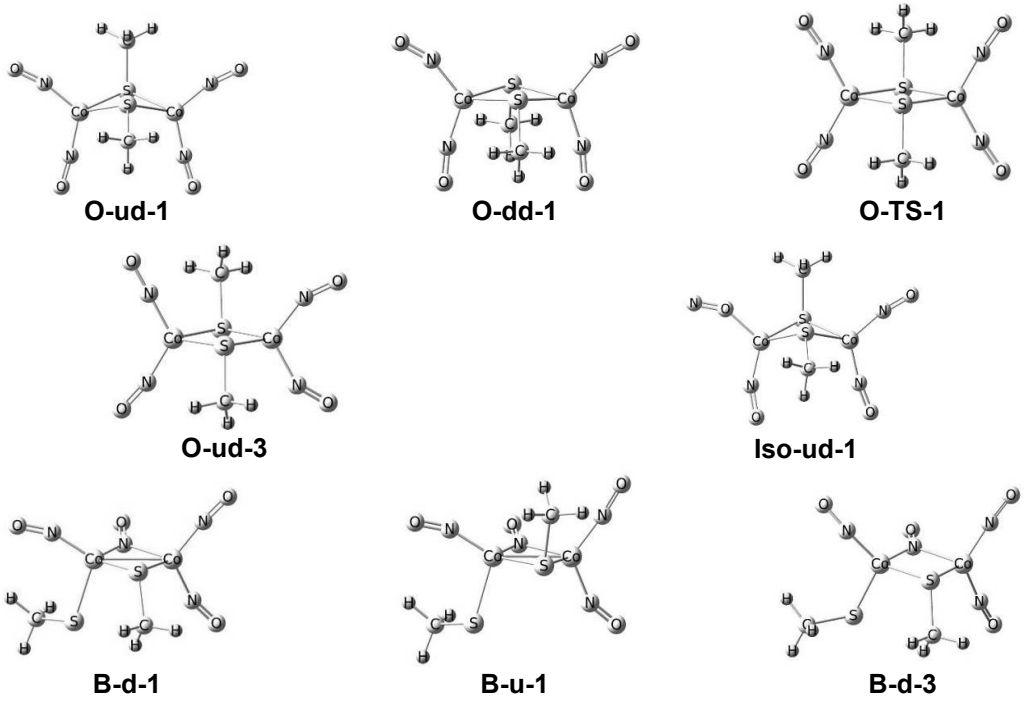

Figure 46 – Selected BP86 optimized $Co_2(NO)_4(SCH_3)_2$ geometries.

In contrast to the results obtained for the related neutral $Fe_2(NO)_4S_2$ (chapter 3.3.2) and $Fe_2(NO)_4(\mu\text{-}SCH_3)_2$ species (chapter 3.2), the M06-L method agrees with the other non-local functional, namely the BP86, and not with the hybrid B3LYP for the

$Co_2(CO)_6(SR)_2$ derivatives. Both BP86 and M06-L predict isoenergetic singlet open structures as the ground state. The corresponding triplet spin state isomers have significantly higher relative energy values (Figure 48).

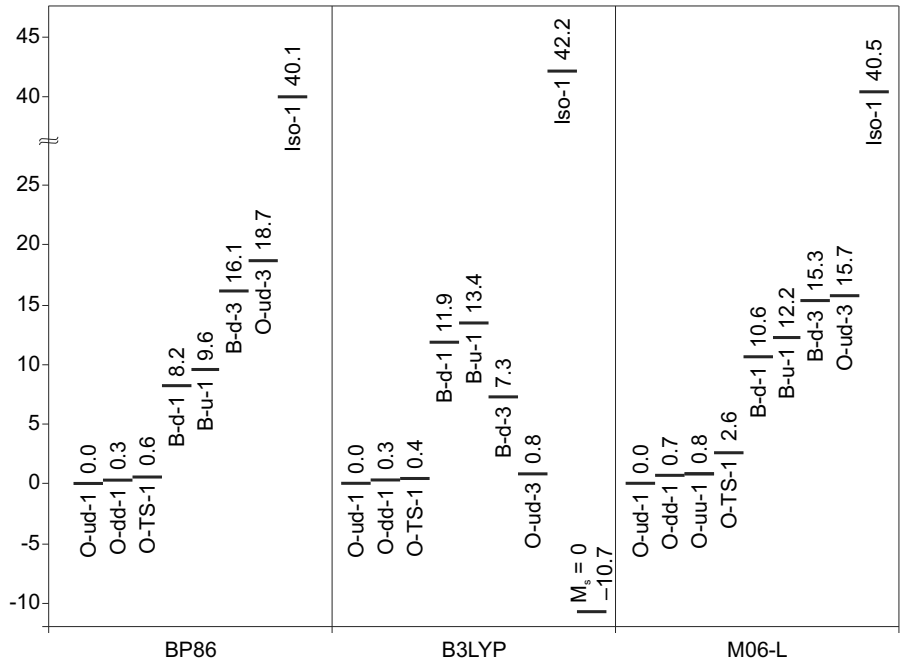

Figure 48 – Relative energies (in kcal mol^{-1}) of the selected optimized $Co_2(NO)_4(SCH_3)_2$ geometries.

Since the M06-L method supports the BP86 results, further discussions will focus only on the data obtained with the later functional, in order to make reasonable comparisons with the related $Co_2(CO)_6(SR)_2$ derivatives discussed earlier. The discussion of the triplet species will also be omitted, because they lie at significantly higher relative energies than the corresponding singlet structures.

For both the $Co_2(NO)_4(SCH_3)_2$ and $Co_2(NO)_4(SCF_3)_2$ derivatives, the lowest energy structures are of the **O-ud-1** open type. The corresponding $Co_2(NO)_4(SCH_3)_2$ and $Co_2(NO)_4(SCF_3)_2$ butterfly structures are both predicted to lie at higher relative energy values than the open $Co_2(NO)_4(SR)_2$ isomers. Furthermore, there is a difference in the relative energy order of the two butterfly structures. This different relative energy trend can be explained by the electrostatic interactions between the terminal sulfur atom and the R substituent of the bridging sulfur (Figure 50). However, the general trends in the relative energies of the respective $Co_2(NO)_4(SCH_3)_2$ and $Co_2(NO)_4(SCF_3)_2$ isomers

remain the same when replacing the electron-releasing CH_3 groups with the electron withdrawing CF_3 groups. The isonitrosyl linkage isomer (**Iso-1**) is predicted by all three functionals to lie with ~40 kcal mol^{-1} above the corresponding global minimum structure.

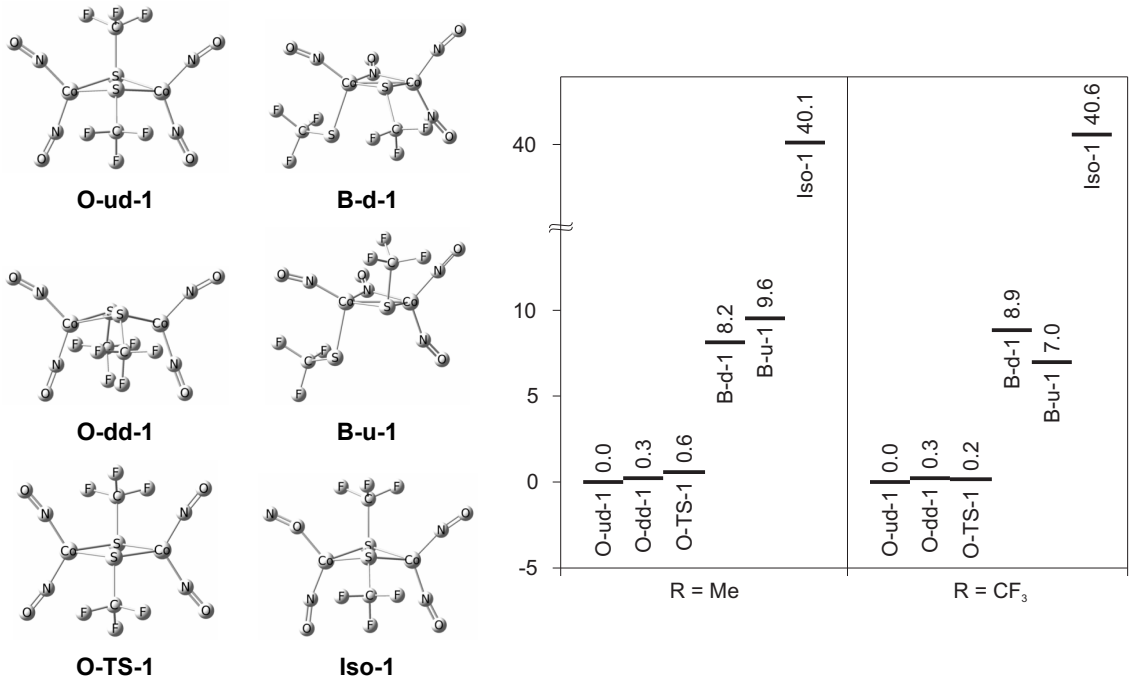

Figure 49 – BP86 optimized $Co_2(NO)_4(\mu\text{-}SCF_3)_2$ geometries and relative energies (in kcal mol^{-1}). The relative energies of the CH_3-substituted species are repeated only for comparison.

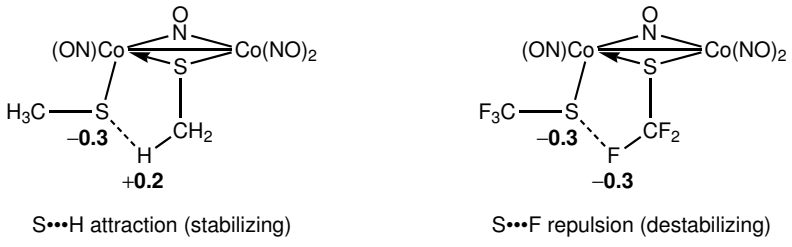

Figure 50 – Electrostatic interactions between the terminal sulfur atom and the R substituent on the bridging sulfur in the $Co_2(NO)_4(SR)_2$ species (R = CH_3, left; R = CF_3, right; natural charges are in **bold**).

The electronic structure of the corresponding $Co_2(NO)_4(SR)_2$ conformers is only weakly influenced by the nature of the SR group. Both the HOMO and the LUMO of the corresponding methyl or trifluoromethyl substituted **O-ud-1** structures have very similar shapes and compositions (Figure 51).

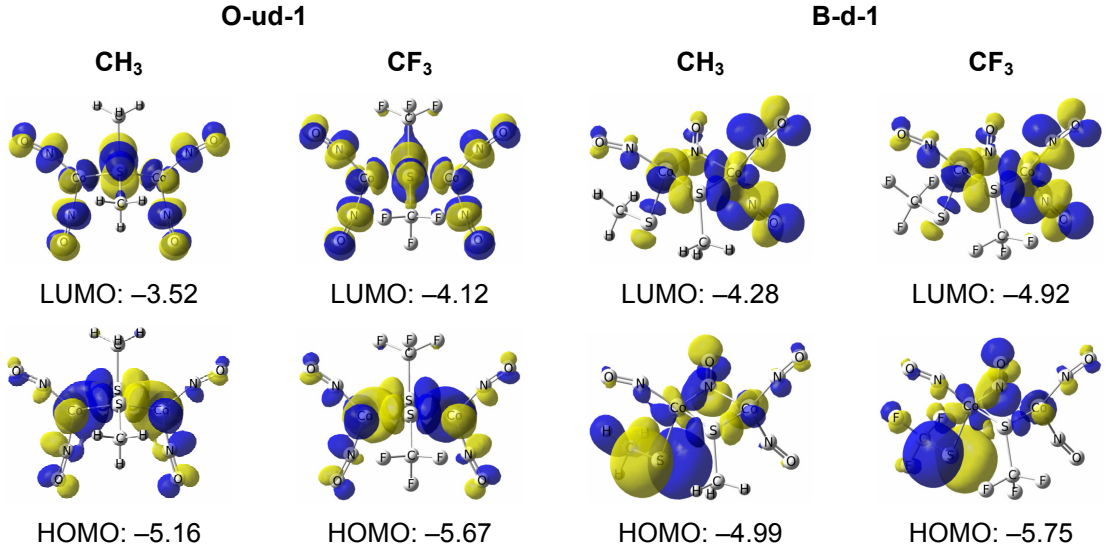

Figure 51 – BP86 energies (eV) and contours at the 0.03 isovalue of the HOMO and LUMO of some relevant $Co_2(NO)_4(SR)_2$ structures (R = CH_3 or CF_3). (positive values: yellow; negative values: blue.)

3.4.3. Conclusions

Density functional calculations on the $Co_2(NO)_4(\mu\text{-}SR)_2$ compounds (R= CH_3, CF_3) predict a highly fluxional system with a preference for structures without a direct Co–Co bond.

The electronic structure of the $Co_2(NO)_4(SR)_2$ conformers is only weakly influenced by the nature of the SR group, as indicated by the similar HOMO/LUMO shapes and compositions of the corresponding methyl or trifluoromethyl substituted open and butterfly structures. On the other hand, the atomic charge distributions of both structure types are noticeably influenced by the nature of the SR group.

4. Unsymmetrical dinuclear rhodium complexes

4.1. Introduction

The experimental Rh···Rh distances in **1** and **2** are at the limit of the sum of the covalent radii of two rhodium atoms, i.e 2.84 Å, which already can be taken as an indication for a strong interaction between the two transition metal centers. However, according to the simple 16 electron rule applied to these systems and the previous theoretical results for similar thiolato-bridged dimeric Rh complexes,[166] one would not expect a single bond between the two rhodium atoms of **1** and **2**. However, a $d_z^2 \rightarrow p^*$ metal-metal interaction, as described for d^8 transition metal dimeric systems,[169] can be present in **1** and **2**. Density functional calculations were carried out to characterize the rhodium-rhodium interactions in these [Rh(μ-S-2-$EPh_2C_6H_4$-κ^2*S*,*E*)$_2$Rh(cod)] compounds.

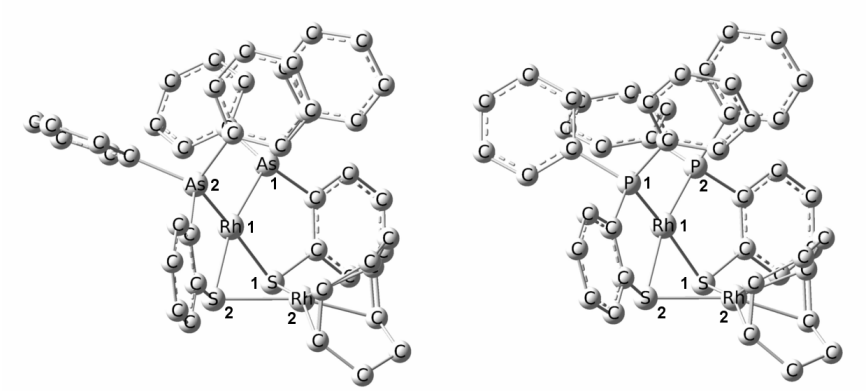

Figure 53 – Solid-state molecular structure of **1** and **2.**

4.2. Theoretical methods

Geometry optimizations in the gas phase were carried out with the Gaussian 09 suite of programs,[26] using the M06-L pure functional[108,109] and using the DZQ basis set recommended by Schultz *et al.*[171] for the rhodium atoms, the standard 6-31G(d) basis for As, P, S and C, and 6-31G for hydrogen. The DZQ basis set uses the relativistic

effective core potentials (ECP) of Stevens *et al.* [172,173,174] along with a valence electron basis set of the (8s8p6d)/[4s4p3d] size.[175]

4.3. Original contributions

Both geometries obtained from the X-ray diffraction data and geometries with the fold angle θ constrained to 180° were optimized. As expected, in both cases the planar forms lie at significantly higher relative energies (Table 27).

Table 27 – Zero-point energy corrected relative energies, calculated Rh···Rh distances and Wiberg bond indices (WBI), for the bent and planar geometries of **1** and **2**.

	Fold angle θ [°]	Rel. E [kcal mol^{-1}]	Rh···Rh [Å]	Rh···Rh WBI
1	99.7 (exp: 105.4)	0	2.837	0.21
	180.00	30.96	3.643	0.06
2	98.5 (exp: 102.6)	0	2.837	0.21
	180.00	30.34	3.614	0.06

Since $d \rightarrow p^*$ donor–acceptor interactions between the two metal atoms have been determined to make the main contribution to bending of these compounds,[169] natural bond orbital (NBO)[29] calculations were carried out in order to identify them (Figure 57). As expected no direct Rh–Rh bonding NBOs were found, which is in agreement with previous theoretical studies for similar thiolato-bridged dimeric Rh complexes.[166]

In the case of the bent structure not only the d_z^2, but also the other *d*-type orbitals interact with the empty p^* lone pairs, and the NBO overlaps are found to be both in-phase and out-of-phase. The planar form of **1** also exhibits similar $d \rightarrow p^*$ donor–acceptor interactions (Figure 57). However, the in-phase $d \rightarrow p^*$ hyperconjugations are clearly predominant in the bent form of **1**, and thus they must play an important role in the stabilization of this structure type.

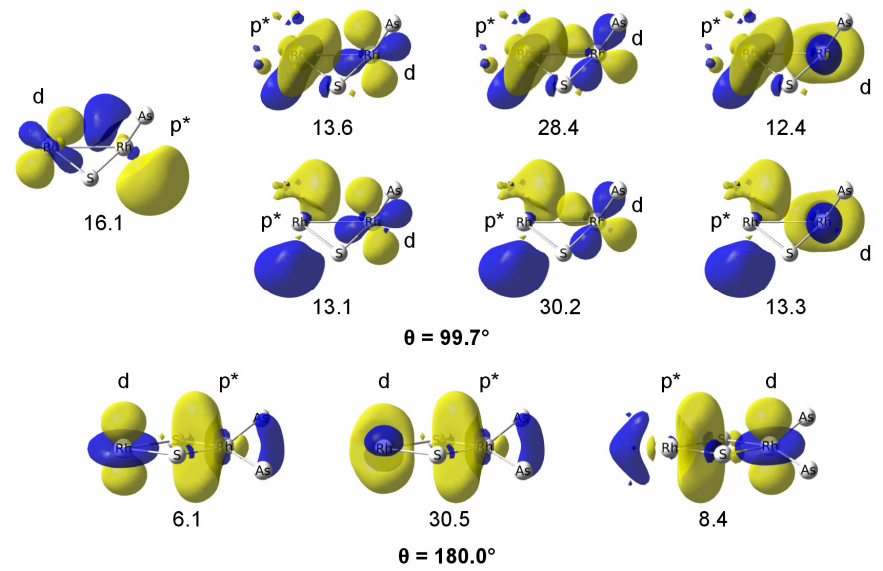

Figure 57 – Contours and second-order energy-lowering values ($\Delta E^{(2)}$, kcal mol^{-1}) of all the identified d → p* hyperconjugations in **1**. Positive values of the orbital contour are represented in yellow (0.05 isovalue) and negative values in blue (–0.05 isovalue).

4.4. Conclusions

Density functional calculations were carried out to characterize the rhodium-rhodium interactions in the dinuclear rhodium complexes [Rh(μ-S-2-EPh$_2$C$_6$H$_4$-κ^2*S*,*E*)$_2$Rh(cod)] (**1**: E = As; **2**: E = P).

The presence of a Rh···Rh interaction was confirmed by natural bond orbital analysis, describeing the Rh···Rh coupling as a $d \rightarrow p^*$ donor–acceptor interactions between the two transition metal atoms.

References

1. P. Kilian, A. M. Z. Slawin, J. D. Woollins, *Chem. Eur. J.*, **2003**, *9*, 215.
2. K. Diemert, W. Kuchen, J. Kutter, *Chem. Ber.*, **1982**, *115*, 1947.
3. T. Mizuta, T. Nakazono, K. Miyoshi, *Angew. Chem. Int. Ed.*, **2002**, *41*, 3897.
4. G. Becker, W. Becker, G. Uhl, W. Uhl, H.-J. Wessely, *Phosphorus Sulfur Relat. Elem.*, **1983**, *18*, 7.
5. G. Becker, W. Becker, O. Mundt, *Phosphorus Sulfur Relat. Elem.*, **1983**, *14*, 267.
6. R. Appel, F. Knoch, H. Kunze, *Chem. Ber.*, **1984**, *117*, 3151.
7. N. Hoa Tran Huy, F. Mathey, *Organometallics*, **1987**, *6*, 207.
8. L. Weber, M. Frebel, R. Boese, *Chem. Ber.*, **1990**, *123*, 733.
9. V. I. Bregadze, *Chem. Rev.*, **1992**, *92*, 209.
10. A search in the CCDC database (August 2011) for unsubstituted 1,2-dicarba-*closo*-dodecaborane(12) structures (*o*-carbaborane) gives 26 C_c–C_c distances in the 1.51–1.71 Å range (mean: 1.63 Å; median: 1.63 Å).
11. A search in the CCDC database (August 2011) for unsubstituted cyclohexa-1,3,5-triene structures gives 7261 C–C distances in the 0.99–1.97 Å range (mean: 1.37 Å; median: 1.38 Å).
12. J. M. Oliva, N. L. Allan, P. von R. Schleyer, C. Viñas, F. Teixidor, *J. Am. Chem. Soc.*, **2005**, *127*, 13538.
13. A. Kreienbrink, M. B. Sárosi, E. G. Rys, P. Lönnecke, E. Hey-Hawkins, *Angew. Chem. Int. Ed.,* **2011**, *50*, 4701.
14. A. Sterzik, E. Rys, S. Blaurock, E. Hey-Hawkins, *Polyhedron*, **2001**, *20*, 3007.
15. S. Stadlbauer, R. Frank, I. Maulana, P. Lönnecke, B. Kirchner, E. Hey-Hawkins, *Inorg. Chem.*, **2009**, *48*, 6072.
16. E. G. Rys, P. Lönnecke, S. Stadlbauer, V. N. Kalinin, E. Hey-Hawkins, *Polyhedron*, **2009**, *28*, 3467.
17. I. Maulana, P. Lönnecke, E. Hey-Hawkins, *Inorg. Chem.*, **2009**, *48*, 8638.
18. J. M. Oliva, C. Viñas, *J. Mol. Struct.,* **2000**, *556*, 33.
19. M. R. Sundberg, R. Uggla, C. Viñas, F. Teixidor, S. Paavola, R. Kivekäs, *Inorg. Chem. Commun.*, **2007**, *10*, 713.
20. A. V. Belyakov, A. Haaland, D. J. Shorokhov, V. I. Sokolov, O. Swang, *J. Mol. Struct.*, **1998**, *445*, 303.
21. M. D. Wodrich, A. Vargas, P.-Y. Morgantini, G. Merino, C. Corminboeuf, *J. Phys. Org. Chem.*, **2009**, *22*, 101.
22. S. Zahn, R. Frank, E. Hey-Hawkins, B. Kirchner, *Chem. Eur. J.,* **2011**, *17*, 6034.
23. P. P. Graczyk, M. Mikolajczyk, in *Topics in Stereochemistry*, E. L. Eliel, S. H. Wilen, Eds., Wiley, New York, **1994**, Vol. 21, p. 159.
24. A. D. Becke, *J. Chem. Phys.*, **1993**, *98*, 5648.
25. C. Lee, W. Yang, R. G. Parr, *Phys. Rev. B*, **1988**, *37*, 785.
26. M. J. Frisch, G. W. Trucks, H. B. Schlegel, G. E. Scuseria, M. A. Robb, J. R. Cheeseman, G. Scalmani, V. Barone, B. Mennucci, G. A. Petersson, H. Nakatsuji, M. Caricato, X. Li, H. P. Hratchian, A. F. Izmaylov, J. Bloino, G. Zheng, J. L. Sonnenberg, M. Hada, M. Ehara, K. Toyota, R. Fukuda, J. Hasegawa, M. Ishida, T. Nakajima, Y. Honda, O. Kitao, H. Nakai, T. Vreven, J. Montgomery, J. A. , J. E. Peralta, F. Ogliaro, M. Bearpark, J. J. Heyd, E. Brothers, K. N. Kudin, V. N. Staroverov, R. Kobayashi, J. Normand, K. Raghavachari, A. Rendell, J. C. Burant, S. S. Iyengar, J. Tomasi, M. Cossi, N. Rega, J. M. Millam, M. Klene, J. E. Knox, J. B. Cross, V. Bakken, C. Adamo, J. Jaramillo, R. Gomperts, R. E. Stratmann, O. Yazyev, A. J. Austin, R. Cammi, C. Pomelli, J. W. Ochterski, R. L. Martin, K. Morokuma, V. G. Zakrzewski, G. A. Voth, P. Salvador, J. J. Dannenberg, S. Dapprich, A. D. Daniels, O. Farkas, J. B. Foresman, J. V. Ortiz, J. Cioslowski, D. J. Fox, *Gaussian 09, Revision A.02*, Gaussian, Inc., Wallingford CT, **2009**.
27. D. Feller, *J. Comput. Chem.*, **1996**, *17*, 1571.
28. K. L. Schuchardt, B. T. Didier, T. Elsethagen, L. Sun, V. Gurumoorthi, J. Chase, J. Li, T. L. Windus, *J. Chem. Inf. Model.*, **2007**, *47*, 1045.

29. A. E. Reed, L. A. Curtiss, F. Weinhold, *Chem. Rev.*, **1988**, *88*, 899.
30. B. Machura, M. Wolff, R. Kruszynski, J. Kusz, *Polyhedron*, **2009**, *28*, 1211.
31. G. Henkel, S. Weißgräber, in *Metal clusters in chemistry*, P. Braunstein, L. A. Oro, P. R. Raithby, Eds., Wiley-VCH: Weinheim, **1999**, p 165.
32. Y. Jean, *Molecular Orbitals of Transition Metal Complexes*, Oxford University Press: New York, **2005**, pp. 29.
33. R. H. Crabtree, *The organometallic chemistry of the transition metals*, John Wiley & Sons: Hoboken, **2005**, pp. 87-89.
34. N. Wiberg, *Lehrbuch der Anorganischen Chemie*, 102 ed., Walter de Gruyter: Berlin, **2007**, pp. 1787-1789.
35. W. Hieber, P. Spacu, *Z. Anorg. Allg. Chem.,* **1937**, *233*, 353.
36. R. B. King, M. B. Bisnette, *Inorg. Chem.*, **1963**, *4*, 1965.
37. R. B. King, *J. Am. Chem. Soc*., **1962**, *84*, 2460.
38. L. F. Dahl, C.-H. Wei, *Inorg. Chem*., **1963**, *2*, 328.
39. R. B. King, *J. Am. Chem. Soc.*, **1963**, *85*, 1584.
40. P. C. Ellgen, J. N. Gerlach*, Inorg. Chem*., **1973,** *12*, 2526.
41. J. Messelhäuseer, I. P. Lorenz, K. Haug, W. Hiller, *Z. Naturforsch*., **1985,** *40b*, 1064.
42. J. W. Tye, M. Y. Darensbourg, M. B. Hall, *Inorg. Chem.,* **2006**, *45*, 1552.
43. M. C. Ortega-Alfaro, N. Hernández, I. Cerna, J. G. López-Cortés, E. Gómez, R. A. Toscano, C. Alvarez-Toledano, *J. Organomet. Chem.,* **2004**, *689*, 885.
44. J. Grobe, F. Kober, *Z. Naturforsch., B: Chem. Sci.,* **1969**, *24b*, 1346.
45. C. H. Wei, L. F. Dahl, *Inorg. Chem.,* **1965**, *4*, 1.
46. W. Hieber, J. Gruber, *Z. Anorg. Allg. Chem.*, **1958**, *296*, 91.
47. D. Seyferth, R. S. Henderson, L. C. Song, *Organometallics,* **1982**, *1*, 125.
48. I. Silaghi-Dumitrescu, T. E. Bitterwolf, R. B. King, *J. Am. Chem. Soc.*, **2006**, *128*, 5342.
49. A. Kramer, I. P. Lorenz, *J. Organomet. Chem*., **1990**, *388*, 187.
50. D. Seyferth, R. S. Henderson, *J. Organomet. Chem*., **1991**, *419*, 113.
51. M. D. Westmeyer, C. P. Galloway, T. B. Rauchfuss, *Inorg. Chem*., **1994**, *33*, 4615.
52. J. Messelhäuser, K. U. Gutenson, I. P. Lorenz, W. Hiller, *J. Organomet. Chem.*, **1987**, *321*, 377.
53. K. M. Flynn, R. A. Bartlett, M. M. Olmstead, P. P. Power, *Organometallics*, **1986**, *5*, 813.
54. R. L. DeKock, E. J. Baerends, R. Hengelmolen, *Organometallics,* **1984**, *3*, 289.
55. J. W. Peters, W. N. Lanzilotta, B. J. Lemon, L. C. Seefeldt, *Science*, **1998**, *282*, 1853.
56. Y. Nicolet, B. J. Lemon, J. C. Fontecilla-Camps, J. W. Peters, *Trends Biochem. Sci,* **2000**, *25*, 138.
57. M. Y. Darensbourg, E. J. Lyon, X. Zhao, I. P. Georgakaki, *Proc. Natl. Acad. Sci. U.S.A.,* **2003**, *100*, 3683.
58. D. Seyferth, G. B. Womack, M. K. Gallagher, M. Cowie, B. W. Hames, J. P. Fackler, A. M. Mazany, *Organometallics,* **1987**, *6*, 283.
59. A. Winter, L. Zsolnai, G. Huttner, *Z. Naturforsch., B: Chem. Sci.,* **1982**, *37*, 1430.
60. E. J. Lyon, I. P. Georgakaki, J. H. Reibenspies, M. Y. Darensbourg, *Angew. Chem. Int. Ed.,* **1999**, *38*, 3178.
61. I. P. Georgakaki, L. M. Thomson, E. J. Lyon, M. B. Hall, M. Y. Darensbourg, *Coord. Chem. Rev.,* **2003**, *238-239*, 255.
62. J. L. Davidson, D. W. A. Sharp, *Dalton Trans*., **1972**, 107.
63. E. Klumpp, L. Markó, G. Bor, *Chem. Ber.,* **1964**, *97*, 926.
64. E. Klumpp, G. Bor, L. Markó, *Chem. Ber.,* **1967**, *100*, 1451.
65. C. H. Wei, L. F. Dahl, *J. Am. Chem. Soc.,* **1968**, *90*, 3960.
66. C. H. Wei, L. F. Dahl, *J. Am. Chem. Soc.,* **1968**, *90*, 3969.
67. C. H. Wei, L. F. Dahl, *J. Am. Chem. Soc.,* **1968**, *90*, 3977.
68. G. Bor, G. Natile, *J. Organomet. Chem.*, **1971**, 2*6*, C33.
69. H. Greenfield, H. W. Sternberg, R. A. Friedel, J. H. Wotiz, R. Markby, I. Wender, *J. Am. Chem. Soc.* **1956**, *78*, 120.
70. R. S. Dickson, P. J. Fraser, *Adv. Organomet. Chem*. **1974**, *12*, 323.
71. M. J. Went, *Adv. Organomet. Chem.* **1997**, *41*, 69.
72. G. Gervasio, S. Vastag, G. Bor, G. Natile, L. Markó, *Inorg. Chim. Acta* **1996**, *251*, 35.
73. R. Minkwitz, H. Borrmann, J. Nowicki, *Z. Naturforsch., B: Chem. Sci.,* **1992**, *47*, 915.

74. G. Li, Q.-S. Li, I. Silaghi-Dumitrescu, R. B. King, H. F. Schaefer III, *Dalton Trans.,* **2009**, 10474.
75. G. Bor, G. Natile, *J. Organomet. Chem.*, **1971**, *26*, C33.
76. O. Heyke, G. Beuter, I.-P. Lorenz, *J. Chem. Soc., Dalton Trans.*, **1992**, 2405.
77. A. Shaver, S. Morris, R. Turrin, V. W. Day, *Inorg. Chem.*, **1990**, *29*, 3622.
78. A. D. Becke, *Physical Review A*, **1988**, *38*, 3098.
79. J. P. Perdew, *Phys. Rev. B*, **1986**, *33*, 8822.
80. F. Furche, J. P. Perdew, *J. Chem. Phys.*, **2006,** *124*, 044103.
81. M. Zhou, L. Andrews, C. W. Bauschlicher, *Chem. Rev.*, **2001**, *101*, 1931.
82. S. G. Andrade, L. C. S. Gonçalves, F. E. Jorge, *J. Mol. Struc.-THEOCHEM*, **2008**, *864*, 20.
83. R. Ditchfield, W. Hehre, J. A. Pople, *J. Chem. Phys.*, **1971**, *54*, 724.
84. A. J. H. Wachters, *J. Chem. Phys*., **1970**, *52*, 1033.
85. J. C. W. Bauschlicher, S. R. Langhoff, H. Partiidge, L. A. Barnes, *J. Chem. Phys.*, **1989**, *91*, 2399.
86. T. H. Dunning, Jr., P. J. Hay, in *Modern Theoretical Chemistry*, H. F. Schaefer, III, ed., Plenum, New York, **1976**, Vol. 3, p. 1.
87. M. J. Frisch, G. W. Trucks, H. B. Schlegel, G. E. Scuseria, M. A. Robb, J. R. Cheeseman, J. J. A. Montgomery, T. Vreven, K. N. Kudin, J. C. Burant, J. M. Millam, S. S. Iyengar, J. Tomasi, V. Barone, B. Mennucci, M. Cossi, G. Scalmani, N. Rega, G. A. Petersson, H. Nakatsuji, M. Hada, M. Ehara, K. Toyota, R. Fukuda, J. Hasegawa, M. Ishida, T. Nakajima, Y. Honda, O. Kitao, H. Nakai, M. Klene, X. Li, J. E. Knox, H. P. Hratchian, J. B. Cross, C. Adamo, J. Jaramillo, R. Gomperts, R. E. Stratmann, O. Yazyev, A. J. Austin, R. Cammi, C. Pomelli, J. W. Ochterski, P. Y. Ayala, K. Morokuma, G. A. Voth, P. Salvador, J. J. Dannenberg, V. G. Zakrzewski, S. Dapprich, A. D. Daniels, M. C. Strain, O. Farkas, D. K. Malick, A. D. Rabuck, K. Raghavachari, J. B. Foresman, J. V. Ortiz, Q. Cui, A. G. Baboul, S. Clifford, J. Cioslowski, B. B. Stefanov, G. Liu, A. Liashenko, P. Piskorz, I. Komaromi, R. L. Martin, D. J. Fox, T. Keith, M. A. Al-Laham, C. Y. Peng, A. Nanayakkara, M. Challacombe, P. M. W. Gill, B. Johnson, W. Chen, M. W. Wong, C. Gonzalez, J. A. Pople *Gaussian 03*, *Revision B.02*; Gaussian, Inc., Pittsburgh PA, **2003**.
88. ***Spartan'06*** Wavefunction, Inc. Irvine, CA.
89. Z. Zhang, Q.-s. Li, Y. Xie, R. B. King, H. F. Schaefer III, *Inorg. Chem.,* **2009**, *48*, 6167.
90. B. N. Papas, H. F. Schaefer III, *J. Mol. Struc.-THEOCHEM*, **2006**, *768*, 175.
91. H. Jacobsen, T. Ziegler, *J. Am. Chem. Soc.*, **1996**, *118*, 4631.
92. J. M. L. Martin, C. W. Bauschlicher, A. Ricca, *Comput. Phys. Commun.*, **2001**, *133*, 189.
93. A. R. Butler, D. L. H. Williams, *Chem. Soc. Rev.*, **1993**, *22*, 233.
94. T. W. Hayton, P. Legzdins, W. B. Sharp, *Chem. Rev.*, **2002**, *102*, 935.
95. A. R. Butler, C. Glidewell, M.-H. Li, in *Adv. Inorg. Chem.*, A. G. Sykes, Ed., Academic Press, London, **1988**, Vol. 32, p. 335.
96. J. A. McCleverty, *Chem. Rev.,* **2004**, *104*, 403.
97. B. Machura, *Coord. Chem. Rev.,* **2005**, *249*, 2277.
98. B. L. Wescott, J. H. Enemark, in *Inorganic Electronic Structure and Spectroscopy*, A. B. P. Lever, E.I. Solomon, Eds., Wiley and Sons, New York, **1999**, Vol. 2, p. 403.
99. C. A. Brown, M. A. Pavlosky, T. E. Westre, Y. Zhang, B. Hedman, K. O. Hodgson, E. I. Solomon, *J. Am. Chem. Soc.*, **1995**, *117*, 715.
100. F. Neese, *J. Biol. Inorg. Chem.* **2006**, *11*, 702.
101. K. H. Hopmann, J. Conradie, A. Ghosh, *J. Phys. Chem. B*, **2009**, *113*, 10540.
102. R. Silaghi-Dumitrescu, I. Silaghi-Dumitrescu, *J. Inorg. Biochem.* **2006**, *100*, 161.
103. A. Ghosh, *J. Biol. Inorg. Chem.*, **2006**, *11*, 712.
104. J. P. Perdew, K. Schmidt, in *Density Functional Theory and Its Applications to Materials*; V. E. Van Doren, K. Van Alsenoy, P. Geerlings, *eds.*; American Institute of Physics: Melville, NY, **2001**.
105. I. Silaghi-Dumitrescu, T. E. Bitterwolf, R. B. King, *J. Am. Chem. Soc.*, **2006**, *128*, 5342.
106. M. Radoń, E. Broclawik, K. Pierloot, *J. Phys. Chem. B*, **2010**, *114*, 1518.
107. M. Jaworska, Z. Stasicka, *New J. Chem.* **2005**, *29*, 604.
108. N. Sanina, N. Emel'yanova, A. Chekhlov, A. Shestakov, I. Sulimenkov, S. Aldoshin, *Russ. Chem. Bull.*, **2010**, *59*, 1126.
109. Y. Zhao, D. G. Truhlar, *J. Chem. Phys.,* **2006**, *125*, 194101.
110. Y. Zhao, D. G. Truhlar, *Acc. Chem. Res.,* **2008**, *41*, 157.
111. Y. Zeng, S. Wang, H. Feng, Y. Xie, R. B. King, H. F. Schaefer III, *New J. Chem.,* **2011**, *35*, 920.

112. R. Valero, R. Costa, I. d. P. R. Moreira, D. G. Truhlar, F. Illas, *J. Chem. Phys.*, **2008**, *128*, 114103.
113. V. Bachler, G. Olbrich, F. Neese, K. Wieghardt, *Inorg. Chem.*, **2002**, *41*, 4179.
114. R. Seeger, J. A. Pople, *J. Chem. Phys.*, **1977**, *66*, 3045.
115. G. Schenk, M. Y. Pau, E. I. Solomon, *J. Am. Chem. Soc.*, **2004**, *126*, 505.
116. P. J. Linstrom, W. G. Mallard (Eds.), NIST Chemistry WebBook, NIST Standard Reference Database Number 69, National Institute of Standards and Technology, Gaithersburg, MD, June 2005. Available from: <http://webbook.nist.gov>.
117. A. Shestakov, Y. Shul'ga, N. Emel'yanova, N. Sanina, S. Aldoshin, *Russ. Chem. Bull.*, **2006**, *55*, 2133.
118. M. Güell, J. M. Luis, M. Solà, M. Swart, *J. Phys. Chem. A*, **2008**, *112*, 6384.
119. F. Z. Roussin, *Ann. Chim. Phys.*, **1858**, *52*, 285.
120. A. R. Butler., *J. Chem. Ed.* **1982**, *58*, 549.
121. L. Xianti, Z. An, L. Shanhuo, H. Jinling, L. Jiaxi, *Jiegou Huaxue (Chin. J. Struct. Chem.)*, **1982**, *1*, 79.
122. D. Seyferth, M. K. Gallagher, *J. Organomet. Chem.*, **1981**, *218*, C5.
123. W. Beck, R. Grenz, F. Götzfried, E. Vilsmaier, *Chem. Ber.*, **1981**, *114*, 3184.
124. T. B. Rauchfuss, T. D. Weatherill, *Inorg. Chem.*, **1982**, *21*, 827.
125. C. Glidewell, M. E. Harman, M. B. Hursthouse, I. L. Johnson, M. Motevalli, *J. Chem. Res.*, **1988**, *212*, 1676.
126. A. R. Butler, I. L. Megson, *Chem. Rev.*, **2002**, *102*, 1155.
127. A. Dobry, F. Boyer, *Ann. Inst. Pasteur*, **1945**, *71*, 455.
128. C. S. Yang, *Cancer Res.*, **1980**, *40*, 2633.
129. Z. Wen-Xin, X. Meng-Shan, W. Guang-Hui, W. Ming-Yao, *Cancer Res.*, **1983**, *43*, 339.
130. R. B. King, T. E. Bitterwolf, *Coord. Chem. Rev.*, **2000**, *206–207*, 563.
131. J. T. Thomas, J. H. Robertson, E. G. Cox, *Acta Cryst.*, **1958**, *11*, 599.
132. M. Lewin, K. Fisher, I. Dance, *Chem. Comm.*, **2000**, 947.
133. D. Seyferth, M. K. Gallagher, M. Cowie, *Organometallics*, **1986**, *5*, 539.
134. S. S. Sung, C. Glidewell, A. R. Butler, R. Hoffmann, *Inorg. Chem.*, **1985**, *24*, 3856.
135. L. Noodleman, C. Y. Peng, D. A. Case, J. M. Mouesca, *Coord. Chem. Rev.*, **1995**, *144*, 199.
136. L. Noodleman, T. Lovell, T. Liu, F. Himo, R. A. Torres, *Curr. Opin. Chem. Biol.*, **2002**, *6*, 259.
137. R. A. Torres, T. Lovell, L. Noodleman, D. A. Case, *J. Am. Chem. Soc.*, **2003**, *125*, 1923.
138. N. Sanina, O. Filipenko, S. Aldoshin, N. Ovanesyana, *Russ. Chem. Bull.*, **2000**, *49*, 1109.
139. M.-L. Tsai, W.-F. Liaw, *Inorg. Chem.*, **2006**, *45*, 6583.
140. T.-T. Lu, C.-C. Tsou, H.-W. Huang, I. J. Hsu, J.-M. Chen, T.-S. Kuo, Y. Wang, W.-F. Liaw, *Inorg. Chem.*, **2008**, *47*, 6040.
141. R. Wang, M. A. Camacho-Fernandez, W. Xu, J. Zhang, L. Li, *J. Chem. Soc., Dalton Trans.*, **2009**, 777.
142. J. H. Enemark, R. D. Feltham, *Coord. Chem. Rev.*, **1974**, *13*, 339.
143. N. Sanina, I. Chuev, S. Aldoshin, N. Ovanesyan, V. Strelets, Y. Geletii, *Russ. Chem. Bull.*, **2000**, *49*, 444.
144. N. A. Sanina, S. M. Aldoshin, *Russ. Chem. Bull.*, **2004**, *53*, 2428.
145. F. Neese, *Coord. Chem. Rev.*, **2009**, *253*, 526.
146. M. Reiher, O. Salomon, B. Artur Hess, *Theor. Chem. Acc.*, **2001**, *107*, 48.
147. K. H. Hopmann, L. Noodleman, A. Ghosh, *Chem. Eur. J.*, **2010**, *16*, 10397.
148. G. Aullón, P. Alemany, S. Alvarez, *J. Organomet. Chem.*, **1994**, *478*, 75.
149. S. Alvarez, A. A. Palacios, G. Aullón, *Coord. Chem. Rev.*, **1999**, *185-186*, 431.
150. W. Manchot, H. Gall, *Ber. Dtsch. Chem. Ges.*, **1927**, *60*, 2318.
151. W. Manchot, F. Kaess, *Ber. Dtsch. Chem. Ges.*, **1927**, *60*, 2175.
152. W. Hieber, I. Bauer, G. Neumair, *Z. Anorg. Allg. Chem.*, **1965**, *335*, 250.
153. W. Hieber, R. Marin, *Z. Anorg. Allg. Chem.*, **1939**, *240*, 241.
154. W. Hieber, J. Ellermann, *Chem. Ber.*, **1963**, *96*, 1650.
155. P. Bladon, M. Dekker, G. R. Knox, D. Willison, G. A. Jaffari, R. J. Doedens, K. W. Muir, *Organometallics*, **1993**, *12*, 1725.
156. T. E. Bitterwolf, P. Pal, *Inorg. Chim. Acta*, **2006**, *359*, 1501.
157. A. Bader, E. Linder, *Coord. Chem. Rev.*, **1991**, *108*, 27.

158. J. R. Dilworth, N. Wheatley, *Coord. Chem. Rev.*, **2000**, *199*, 89.
159. C. S. Slone, D. A. Weinberger, C. A. Mirkin, *Prog. Inorg. Chem*., **1999**, *48*, 233.
160. P. Braunstein, F. Naud, *Angew. Chem., Int. Ed. Engl*., **2001**, *40*, 680.
161. G. D. Figuly, C. K. Loop, J. C. Martin, *J. Am. Chem. Soc.*, **1989**, *111*, 654.
162. E. Block, V. Eswarakrishnan, M. Gernon, G. Ofori-Okai, C. Saha, K. Tang, J. Zubieta*, J. Am. Chem. Soc.*, **1989**, *111*, 658.
163. K. Smith, C. M. Lindsay, G. J. Pritchard, *J. Am. Chem. Soc.*, **1989**, *111***,** 665.
164. E. Block, G. Ofori-Okai, J. Zubieta, *J. Am. Chem. Soc.***, 1989**, *111*, 2327.
165. A. Hildebrand, M. B. Sárosi, P. Lönnecke, L. Silaghi-Dumitrescu, E. Hey-Hawkins, *Rev. Roum. Chim.,* **2010**, *55*, 885.
166. A search in the CCDC database (August 2011) for unsubstituted sulfur bridged dimeric rhodium complexes gives 248 Rh···Rh distances in the 2.55–3.78 Å range (mean: 3.25 Å; median: 3.24 Å).
167. A. M. Masdeu, A. Ruiz, S. Castillón, C. Claver, P. B. Hitchcock, P. A. Chaloner, C. Bó, J. M. Poblet, P. Sarasa, *J. Chem. Soc. Dalton Trans*, **1993**, 2689.
168. G. Aullón, G. Ujaque, A. Lledós, S. Alvarez, P. Alemany, *Inorg. Chem*., **1998**, *37*, 804.
169. J. Novoa, G. Aullón, P. Alemany, S. Alvarez, *J. Am. Chem. Soc*., **1995**, *117*,7169.
170. G. Aullón, P. Alemany, S. Alvarez, *Inorg. Chem*., 1996, **35**, 5061.
171. P. Hofmann, C. Meier, W. Hiller, M. Heckel, J. Riede, M. U. Schmidt, *J. Organomet. Chem*., 1995, **490**, 51.
172. N. E. Schultz, Y. Zhao, D. G. Truhlar, *J. Phys. Chem. A*, **2005**, *109*, 11127.
173. W. J. Stevens, H. Basch, M. Krauss, *J. Chem. Phys.*, **1984**, *81*, 6026.
174. W. J. Stevens, M. Krauss, H. Basch, P. G. Jasien, *Can. J. Chem.*, **1992**, *70*, 612.
175. T. R. Cundari, W. J. Stevens, *J. Chem. Phys.*, **1993**, *98*, 5555.
176. N. E. Schultz, Y. Zhao, D. G.Truhlar, *J. Phys. Chem. A*, **2005**, *109*, 4388.
177. K. B. Wiberg, *Tetrahedron*, **1968**, *24*, 1083.
178. G. Aullón, G. Ujaque, A. Lledós, S. Alvarez, P. Alemany, *Inorg. Chem*., **1998**, *37*, 804.